CrossMark

ORIGINAL ARTICLE

Inducible expression of magnesium protoporphyrin chelatase subunit I (CHLI)-amiRNA provides insights into cucumber mosaic virus Y satellite RNA-induced chlorosis symptoms

Sachin Ashok Bhor[1] · Chika Tateda[2] · Tomofumi Mochizuki[3] ·
Ken-Taro Sekine[2,4] · Takashi Yaeno[1,5,6] · Naoto Yamaoka[1,5] ·
Masamichi Nishiguchi[5] · Kappei Kobayashi[1,5,6]

Abstract Recent studies with Y satellite RNA (Y-sat) of cucumber mosaic virus have demonstrated that Y-sat modifies the disease symptoms in specific host plants through the silencing of the magnesium protoporphyrin chelatase I subunit (CHLI), which is directed by the Y-sat derived siRNA. Along with the development of peculiar yellow phenotypes, a drastic decrease in CHLI-transcripts and a higher accumulation of Y-sat derived siRNA were observed. To investigate the molecular mechanisms underlying the Y-sat—induced chlorosis, especially whether or not the reduced expression of CHLI causes the chlorosis simply through the reduced production of chlorophyll or it triggers some other mechanisms leading to the chlorosis, we have established a new experimental system with an inducible silencing mechanism. This system involves the expression of artificial microRNAs targeting of *Nicotiana tabacum* CHLI gene under the control of chemically inducible promoter. The CHLI mRNA levels and total chlorophyll content decreased significantly in 2 days, enabling us to analyze early events in induced chlorosis and temporary changes therein. This study revealed that the silencing of CHLI did not only result in the decreased chlorophyll content but also lead to the downregulation of chloroplast and photosynthesis-related genes expression and the upregulation of defense-related genes. Based on these results, we propose that the reduced expression of CHLI could activate unidentified signaling pathways that lead plants to chlorosis.

Introduction

Plant viruses and viroids infect plants systemically and induce a spectrum of symptoms, including chlorosis and necrosis in localized and spread areas of the infected plants. These symptoms are very specific to a combination of the host and the virus. The mechanism of host-virus interaction responsible for such phenotypic changes has largely remained to be elucidated, although it evidently alters the morphological and physiological aspects of host plant cells including the reduced chlorophyll content, and the impaired chloroplast structure and function. The disturbance of chloroplast functions may be responsible for the production of chlorosis that is associated with virus infection [19]. Several plant-virus interaction studies have revealed that virus infection inhibits host photosynthesis, which is usually accompanied by viral symptoms [7, 9, 10, 16, 29]. Virus infection commonly causes

✉ Kappei Kobayashi
  kappei@ehime-u.ac.jp

1 The United Graduate School of Agricultural Sciences, Ehime University, Matsuyama, Ehime 790-8566, Japan

2 Iwate Biotechnology Research Center, Kitakami, Iwate 024-0003, Japan

3 Graduate School of Life and Environmental Sciences, Osaka Prefecture University, Sakai, Osaka 599-8531, Japan

4 Present Address: Faculty of Agriculture, University of the Ryukyus, Nakagami, Okinawa 903-0213, Japan

5 Faculty of Agriculture, Ehime University, 3-5-7 Tarumi, Matsuyama, Ehime 790-8566, Japan

6 Research Unit for Citromics, Ehime University, Matsuyama, Ehime 790-8566, Japan

chlorosis resulting into impaired chlorophyll biosynthesis and reduced photosynthetic activities that lead to a decrease in biomass production and significant loss in crop yield [44]. Until now, several attempts have been made to explore the precise molecular mechanisms underlying virally induced chlorosis but with limited success.

The role of different plant-pathogen factors responsible for structural and functional changes in chlorotic tissues of virus-infected plants has been studied. These changes include (1) variation in chlorophyll fluorescence and reduced chlorophyll content [3], (2) inhibition of photosynthetic activity [17], (3) disproportionate accumulation of photoassimilates [1, 23], (4) alterations in chloroplast ultrastructure and functions [4, 25], (5) downregulation of nuclear-encoded chloroplast and photosynthesis-related genes and proteins (CPRGs and CPRPs, respectively) [8, 21, 34, 35], (6) direct binding of viral components with chloroplast factors [4, 33], and (7) perturbation of photosynthesis by regulation of host miRNA expression [43].

Viroids are smallest infectious agents having small, noncoding, highly structured genome. A similar type of RNA molecules, viral satellite RNAs, although lacking the ability to replicate autonomously, have also been described to have pathogenic roles. Despite their non-coding small genome, they can induce disease symptoms in host plants ranging from chlorosis and necrosis to complete death of infected plant [13]. Recent studies have shown that viroids and viral satellite RNAs can exploit host RNA-silencing machinery to modulate the viral disease symptom through the downregulation of CPRGs. Peach latent mosaic viroid (PLMVd) infects its natural host peach and causes albinism by depletion of chloroplast-targeted heat shock protein 90 (Hsp90C) through RNA interference mechanism [22]. A similar mechanism was reported in the pathogenesis of Y satellite RNA (Y-sat) of cucumber mosaic virus (CMV) in 14 species of *Nicotiana* plants including *Nicotiana tabacum* by two different research groups [34, 35]. These studies clearly demonstrated that the gene encoding subunit I (CHLI) of magnesium protoporphyrin chelatase (Mg-chelatase), a chlorophyll biosynthetic enzyme, is involved in the development of unique yellow phenotypes in plants infected with CMV harboring Y-sat. Along with the induction of yellow phenotypes, a drastic decrease in CHLI mRNA level and a high-level accumulation of Y-sat derived siRNA were observed. Similar yellow phenotypes were observed in *Arabidopsis thaliana* (*AtchlI*) [30], *Zea mays* L. (*ZmchlI*) [31] mutants and CHLI-silenced transgenic tobacco plants [26].

Although all these studies suggest that the reduced expression of CHLI gene led to a peculiar yellow phenotype or chlorosis, it is still an open question whether the reduced expression of CHLI causes the chlorosis simply through the reduced production of chlorophyll or it triggers some other mechanisms leading to the chlorosis. Papenbrock et al. [26] demonstrated the reduced accumulation of light-harvesting chlorophyll-binding (LHC) proteins in transgenic tobacco lines with reduced Mg-chelatase activities. Those transgenic plants are, however, likely to have reduced Mg-chelatase activities since their germination and therefore, the reduced accumulation of LHC proteins could be attributed to a long-term effect of low Mg-chelatase activity during the development of plants. By contrast, in the case of virus-induced chlorosis, the development of chlorosis is likely to occur during shorter stretches of time. It is important to analyze the progression of chlorosis after the reduction of CHLI expression in normally growing plants.

To address this question, we have established an experimental system to analyze the progress of chlorosis induced by the reduced CHLI gene expression. To this end, we employed artificial microRNAs (amiRNAs) designed to target CHLI mRNA and chemically inducible promoter. In this system, chlorosis could be induced in transgenic tobacco plants as in the previously reported inducible chlorosis systems, in which CaMV Tav [41, 42] and hairpin RNA of Hsp90C [5] are expressed in a chemical-inducible manner. The present system enabled us to analyze early events and temporary changes therein, revealing that CHLI silencing did not only resulted in the decreased chlorophyll content but also caused downregulation of CPRGs expression. Furthermore, the induced CHLI silencing activated the expression of defense-related genes. Based on these results, we propose that the reduced expression of CHLI could activate unidentified signaling pathways that lead plants to chlorosis.

Materials and methods

Design of CHLI-amiRNAs and construction of their inducible plant expression vectors

To generate an endogenous stem-loop backbone for the amiRNA transgenes, we selected widely used *Arabidopsis thaliana* miR319a precursor (AtmiR319a; Accession no. NR_142347). Initially, the 665 and 1586 bp fragments encompassing AtmiR319a precursor sequence were PCR amplified using genomic DNA as a template with two primer pairs, AtM319-845F and AtM319-1510R, and AtM319-499F and AtM319-2085R (Table S1), respectively. A 433 bp DNA fragment including the AtmiR319a precursor gene was amplified from the initial PCR products as a template by PCR using primers SsSl-M319F and M319-BlnR (Table S1) introducing *Sal*I and *Bln*I restriction sites at upstream and downstream, respectively. The PCR product was cloned into Zero Blunt TOPO PCR

cloning vector (Thermo Fisher Scientific, Yokohama, Japan) and sequenced, to give rise to the backbone vector pCRAtmir319-clone4.

Web microRNA Designer (WMD3) (http://wmd3.weigelworld.org/cgi-bin/webapp.cgi) [24, 32] was used to design 21 nucleotides (-nt) amiRNA sequences targeting NtCHLI mRNA (GenBank Accession no. NM_001324838). Two best candidates of amiRNAs, CHLI-ami-1 and -2, suggested by the web service were selected and constructed. The constructs for amiRNAs that target CHLI mRNA was engineered by replacing the 21-nt regions of the natural AtmiR319 miRNA and its partially complementary sequence (miRNA*) by recombinant PCRs as described in WMD3 website. All PCRs were performed with GXL DNA Polymerase (Takara Bio, Kusatsu, Japan) in a volume of 25 μl according to the manufacturer's recommendation. The primer information and PCR protocols are given in Table S1 and S2, respectively. The CHLI-ami-1 and -2 fusion PCR products of 592 and 590 bp were gel purified, cloned into Zero Blunt TOPO PCR cloning vector, verified for sequences, excised with *Sal*I and *Bln*I (Takara Bio) and ligated into the Dexamethasone (Dex)-inducible binary vector pTA7200 [2] at *Xho*I and *Spe*I sites, resulting into pGVG-CHLI-ami-1 and -2, respectively. Both amiRNA plant expression vectors were transformed into *Agrobacterium tumefaciens* strains GV3101.

Generation of transgenic tobacco lines expressing CHLI-ami-1 and -2

The leaf discs from *N. tabacum* cv. SR1 plants, aseptically grown on MS medium containing 0.8% agar without any vitamin or plant hormone were used as an explant. Agrobacterium-mediated transformation of tobacco leaf discs with *A. tumefaciens* harboring pGVG-CHLI-ami-1 and -2 was carried out according to Horsch et al. [12]. The primary transformants were selected on MS medium supplemented with 50 μg/mL hygromycin B (Hyg). All regenerated T_0 transgenic plants were genotyped for the presence of the transgene by PCR with GVGproF1 (5′-CCCTTCCTCTATATAAGGAA-3′) and GVGterR2 (5′-CTGGTGTGTGTGGGCAATGAAA-3′) primers using Extract-N-Amp Plant PCR Kit (Sigma-Aldrich, Japan) according to the manufacturer's instructions. The PCR positive transgenic plants (T_0) were grown to harvest T_1 generation seeds.

Screening of transgenic lines on selective medium

Mature T_1 seeds from PCR positive T_0 transformants were surface-sterilized and grown on a selective MS medium containing 50 μg/mL Hyg and 20 μg/mL Meropenem with or without 1 μM Dex (Nacalai tesque, Kyoto, Japan). After 2 weeks at 25 °C under the 16/8 h light/dark cycle condition, the phenotype of the T_1 seedlings was observed. The transgenic lines that showed the segregation ratios of 3:1 for Hyg resistance and the chlorosis phenotype in a Dex-dependent manner were selected for T_2 seeds production. The surface sterilized T_2 seeds from the selected transgenic lines were sown onto the same selective MS medium. Two weeks after sowing, the seedlings in the plates were observed for phenotypic changes. T_2 sublines that showed no segregation for Hyg resistance and reproducible Dex-dependent chlorosis were used for the analysis.

Plant growth and induced expression of CHLI-ami-1 and -2

Seedlings of selected T_2 sublines of CHLI-ami-1 and -2 transgenic lines, which were grown on a wet filter paper containing Petri dishes for 1 week, were transferred to Jiffy 7 (Jiffy Products International, Kristiansand, Norway) and grown for additional 2 or 3 weeks. The plants received water on every alternate day with 1000 times diluted Hyponex 6-10-5 (Hyponex Japan, Osaka, Japan) solution once a week. To induce the expression of CHLI-ami-1 and -2, some plants received daily foliar applications of freshly diluted 50 μM Dex solution containing 0.01% (v/v) Tween-20 using a spray bottle, while other plants receive 2% ethanol solution containing 0.01% (v/v) Tween-20 in the same manner as a control (mock) treatment. The transgenic plants were monitored daily for the visible phenotypic changes and photographed. Also, leaf samples were collected for biochemical and molecular analyses at indicated days post-treatment (dpt).

Determination of total chlorophyll content

The leaf samples were collected for quantifying total chlorophyll content at 0 (before Dex treatment), 2, 5 and 7 dpt (Dex and mock treatments). Leaf tissues of about 100 mg were cut out from the leaf blade, weighed, frozen in liquid nitrogen in a centrifuge tube containing two 5 mm stainless steel beads, and ground to a fine powder by using tissue homogenizer (Microsmash; Tomy, Tokyo, Japan). 1 mL of 99.5% methanol was added to the powdered leaf tissue, mixed well with vortex, and centrifuged at 12,000 rpm for 10 min at 4 °C to extract the pigments in leaf tissues. The supernatant was collected in a fresh tube and measured for the absorbance at 652, 665.2, and 750 nm using a spectrophotometer (UV-1800; Shimadzu, Kyoto, Japan). The total chlorophyll (a + b) content (μg/mg fresh mass of leaf tissues) was calculated as suggested by Porra et al. [27].

Quantitative real time-PCR

The leaf samples for total RNA extraction was collected at 2 dpt. About 100 mg of leaf tissues ground to the fine powder as described before. Total RNA was extracted using Sepasol-RNA I Super G (Nacalai Tesque, Inc., Kyoto, Japan) as described previously [42]. In order to remove the co-extracted genomic DNA from total RNA preparations, about 10 μg of total RNA was treated with the RNase-free recombinant DNase I (Takara Bio) in the presence of recombinant ribonuclease inhibitor (Takara Bio) followed by purification using Sepasol-RNA I Super G. Reverse transcription was performed with 2 μg total RNA using M-MuLV reverse transcriptase (New England Biolabs, Tokyo, Japan) with 50 pmol/μl random hexamer primer. For the expression analysis of pathogenesis-related genes and photosynthetic genes, primers for qRT-PCR analysis (Table S3) were designed using IDT online qPCR primer designing tool (https://sg.idtdna.com/Primerquest/Home/Index). PCR amplification was carried out with KAPA SYBR FAST qPCR master mix (Nippon Genetics, Tokyo, Japan) using an Applied Biosystems StepOnePlus Real-Time PCR apparatus (Applied Biosystems, USA) under the condition as follows: 95 °C for 20 s, 40 cycles of 95 °C for 3 s and 60 °C for 30 s, and then 95 °C for 15 s, 60 °C for 1 min, and 95 °C for 15 s for melt curve analysis. Expression levels of all the transcripts were normalized against that of *N. tabacum* EF1α mRNA as an internal reference. The experiments were conducted with three biological replications, and each sample was tested in triplicates. The transcript level of target genes was calculated by comparative C_T ($\Delta\Delta C_T$) method.

Histological analysis

For histological analysis, leaf tissue samples were collected at 7 dpt. Leaf samples were cut into 2 mm × 5 mm pieces and fixed with fixative buffer (4% glutaraldehyde in 60 mM HEPES pH 7.0, and 0.125 M sucrose). After fixing the samples, incubation with Dalton's buffered 1% osmium tetroxide for 2 h at 4 °C was performed. Subsequently, tissues were dehydrated with alcohol series and embedded in Spurr resin (Nisshin EM, Tokyo, Japan). Semi-thin sections (3 μm) were prepared from at least five resin blocks and stained with 0.2% toluidine blue solution and examined under a BX-43 microscope (Olympus, Tokyo, Japan).

Results

Establishment of inducible CHLI silencing systems

To establish a system in which the expression of CHLI gene can be silenced in an artificially inducible manner, we employed artificially engineered miRNAs designed based on an endogenous *Arabidopsis* miR319a precursor. Two amiRNAs (CHLI-ami-1 and -2) were predicted to target the same position (nucleotide No. 1332–1352 of NTGI.040111 in *Nicotiana tabacum* EST NtGI-7.0 database) in *N. tabacum* CHLI-mRNA with single nucleotide mismatch at their 5′ end. The CHLI-ami-1 has a mismatch at 17th (C–C) nucleotide from the 5′ end, and the CHLI-ami-2 has two mismatches at 16th (U–C) and 21st (U–U) nucleotides (Fig. 1a). The sequences corresponding to miRNA and miRNA* in miR319a precursor gene were replaced with those of CHLI-ami-1 or -2 by overlapping PCRs. The resultant DNA fragments of CHLI-ami-1 or -2 were introduced into the Dex-inducible plant expression vector to obtain pGVG-CHLI-ami-1 and -2 binary vectors.

Agrobacterium harboring pGVG-CHLI-ami-1 and -2 binary vectors was used for plant transformation, which brought 14 and 9 transgenic shoots on growth medium containing Hygromycin, respectively. All the primary transformants (T_0) were characterized for the presence of transgenes by PCR (Fig. S1). The PCR positive plants (T_0) were grown to harvest T_1 seeds and the seeds from individual transgenic plants were screened on selective growth medium containing 1 μM Dex. The transgenic seedlings were observed for visible phenotypic changes until 2 weeks, and transgenic lines that showed clear chlorosis were selected for T_2 seeds production.

T_2 seeds from different T_1 plants of each transgenic line were tested for Hyg resistance and chlorosis development on the Dex-containing plates, and homozygous T_2 sublines were selected for further experiments. The non-transformed SR1 seedlings did not show chlorosis symptoms on both Dex-containing and Dex-free plates. The selected T_2 sublines, CHLI-1-11and CHLI-2-8, which harbor CHLI-ami-1 and -2 transgenes respectively, demonstrated the chlorosis phenotypes on Dex-containing plate but not on Dex-free plates, suggesting that the effect of CHLI-amiR-NAs expression are stably inherited among the transgenic lines (Fig. 2). The induced chlorosis phenotype in CHLI-1-11 was milder than those in CHLI-2-8 and iTav-3, which served as a positive control for inducible chlorosis [42].

The CHLI-1-11 and CHLI-2-8 transgenic lines were examined for the expression of CHLI gene with or without Dex-induced expression of amiRNA transgenes. Three-week-old T_2 seedlings from these transgenic lines, non-transformed SR1, transformed control Hsp90C-6 [5], and iTav-3 lines were treated with or without 50 μM Dex. The expression analysis for CHLI-transcripts was performed with samples from 2 dpt. In SR1 and Hsp90C-6, we did not find any change in CHLI expression levels between Dex and mock treatments (Fig. 3). In contrast, a significant decrease in CHLI expression levels was observed in CHLI-amiRNA transgenic lines and iTav-3 (Fig. 3). The results
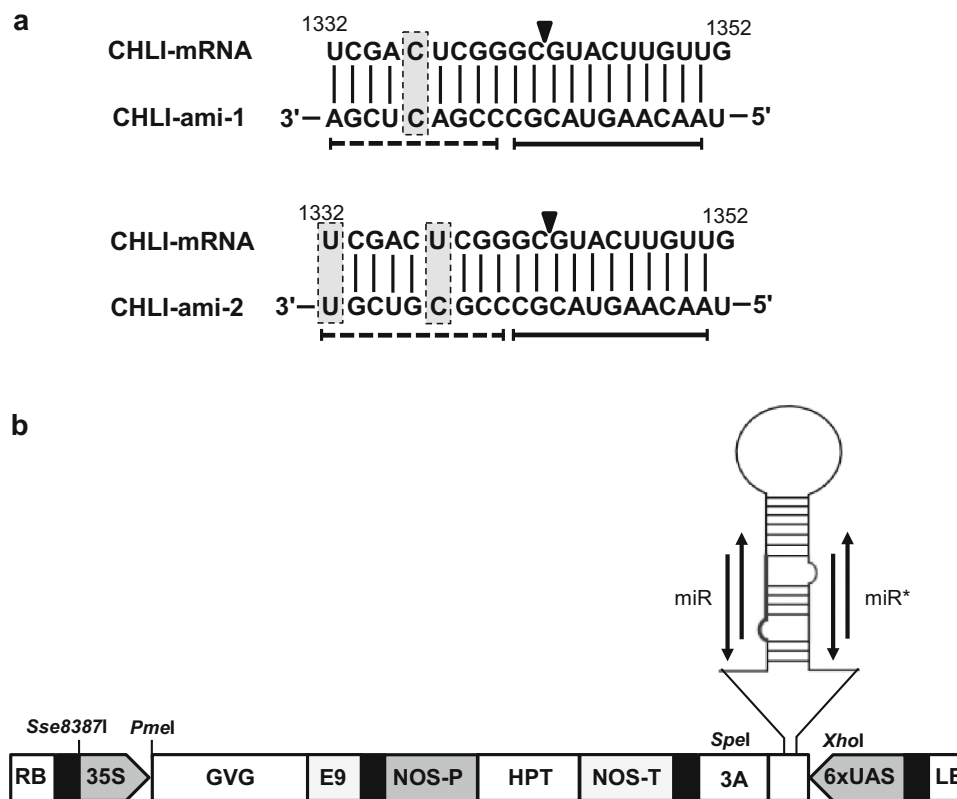
Fig. 1 Predicted mature amiRNAs sequences targeting *N. tabacum* CHLI-mRNA and scheme of constructs for inducible expression of the amiRNAs. **a** Sequences of two amiRNAs (CHLI-ami-1 and -2) that target the same position (nucleotide No. 1332–1352 of NTGI.040111 in *N. tabacum* EST NtGI-7.0 database) in *N. tabacum* CHLI-mRNA. Nucleotide mismatch(es) in CHLI-ami-1 at 17th (C–C) and in CHLI-ami-2 at 16th (U-C) and 21th (U–U) bases are highlighted by *dotted line boxes*, respectively. Predicted cleavage site in CHLI-mRNA is shown by *arrowheads*. The mismatch-sensitive 5′ region (from 2 to 12 nucleotides) of amiRNAs is denoted by *thick lines* below the nucleotides, whereas 3′ region containing mismatch (13–21 nucleotides) is shown by *thick dotted lines*.

b Schematic representation of pGVG-CHLI-ami-1 and -2 vectors used in this study. RB and LB, right and left borders; 6 × UAS, six copies of the GAL4 upstream activating sequence and the −46 to +1 region of the 35S promoter; 426 and 424 bp overlapping PCR products containing CHLI-ami-1 and -2, respectively; 3A, polyadenylation sequence of pea rbcS-3A; NOS-T, nopaline synthase terminator; HPT, hygromycin phosphotransferase gene; NOS-P, *nopaline synthase* gene promoter; E9, polyadenylation sequence of the pea rbcS-E9; GVG, a fusion gene of GAL4-binding domain, VP16 activation domain, and glucocorticoid receptor; 35S, *Cauliflower mosaic virus* 35S promoter

indicate that the Dex-induced expression of CHLI-amiR-NAs successfully silenced the endogenous CHLI genes in CHLI-amiRNA transgenic lines. Downregulation of CHLI expression was also observed in iTav-3 line upon Dex treatment, which is consistent with our previous study, confirming that downregulation of CPRGs is a common phenomenon in virally induced chlorosis and the Tav-induced chlorosis in tobacco [42].

Inducible silencing of CHLI gene expression in transgenic tobacco plants produces chlorosis symptoms

To verify the inducible chlorosis in the aforementioned inducible silencing system, the mock- and Dex-treated plants were monitored until 7 dpt. After Dex treatment, non-transformed SR1 and transformed control Hsp90C-6

plants did not show any phenotypic changes (Fig. 4a, b). Whereas, the Dex-treated iTav, CHLI-1-11, and CHLI-2-8 transgenic lines showed chlorosis with a variable degree (Fig. 4c–e). In addition to this, the mosaic-like phenotype was observed in iTav-3 (Fig. 4f), as reported previously [42]. The chlorosis with patchy patterns with green dots in chlorotic leaf blades was observed in both CHLI-1-11 and CHLI-2-8 transgenic lines (Fig. 4f, g). The transgenic line CHLI-2-8 showed severer chlorosis than CHLI-1-11 (Fig. 4d–g), which is consistent with the results of CHLI expression levels at 2 dpt (Fig. 3).

To elucidate the progression of chlorosis in the inducible CHLI silencing system, the changes in the total chlorophyll content during the development of chlorosis was studied through a time course assay. The total chlorophyll content was determined before Dex treatment (Day 0), and at 2, 5 and 7 dpt of mock and Dex treatments. The visible
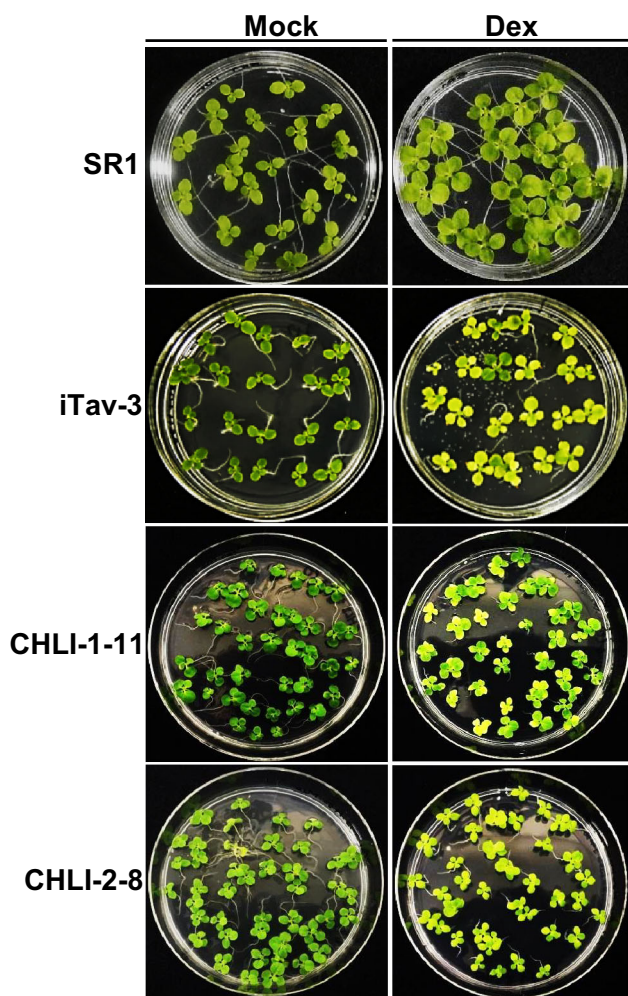
Fig. 2 Development of chlorosis in transgenic seedlings grown on growth medium containing Dex. The seeds from non-transformed control (SR1) were sown on an MS medium (Mock) or a medium containing 1 μM Dex (Dex). T_2 seeds of transgenic lines transgenic lines were sown on a selection medium containing 50 μg/mL Hyg alone (Mock) or a medium containing both 50 μg/mL Hyg and 1 μM Dex (Dex). Previously reported iTav-3 served as a positive control. T_2 seeds from CHLI-1-11 and CHLI-2-8 transgenic lines representing CHLI-ami-1 and -2, respectively were sown on mock and Dex containing media, which exhibited chlorosis with varying degree of severity among the lines. The photographs were taken 2 weeks after sowing (color in print)

chlorosis symptoms were observed in CHLI-amiRNAs transgenic lines only at 5 dpt but not at earlier time points. The statistically significant decrease in total chlorophyll content of iTav-3, CHLI-1-11 and CHLI-2-8 transgenic lines was recorded at 2, 5 and 7 dpt (Fig. 5a). There was no significant change in chlorophyll content in SR1 and Hsp90C-6 lines at any time point. A remarkable decrease in total chlorophyll content in iTav tobacco line during early (between 0 and 2 dpt) and late (between 5 and 7 dpt) stages of chlorosis development was observed (Fig. 5b). In CHLI-1-11 transgenic line, a marked decrease in
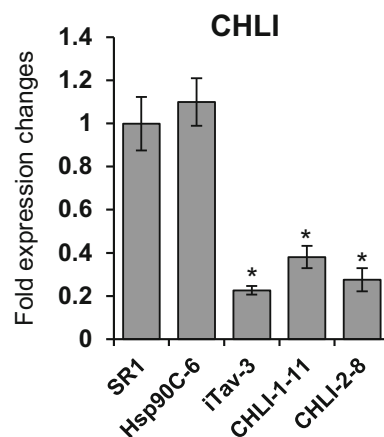

Fig. 3 Expression analysis of CHLI gene by qRT-PCR. Non-transformed control (SR1), control transformant Hsp90C-6, which did not produce any symptom after Dex treatment (Fig. 2), iTav-3 and CHLI-amiRNA transgenic lines (CHLI-1-11 and CHLI-2-8) were analyzed for the relative expression of CHLI gene at 2 dpt with Dex. The expression of target mRNA was normalized to NtEF1α expression. Fold expression changes of the target genes in Dex-treated leaves in comparison with mock-treated were calculated. Bars represent the means ± standard errors for fold change obtained from three replicates per treatment. The asterisks show statistically significant difference between mock- and Dex-treated plants in Student t test ($p < 0.05$)

chlorophyll content was observed during the middle (between 2 and 5 dpt) stage, whereas that in CHLI-2-8 line was observed during middle and late stages. These results suggest that the induced silencing of CHLI gene causes chlorosis to similar extents to iTav-3, although the onset of chlorosis is faster in iTav-3 than in the inducible CHLI silencing lines.

Histological changes in leaf tissues during the chlorosis induced by CHLI amiRNA

The leaf tissues from mock- and Dex-treated CHLI-amiRNA expressing transgenic plants and non-transformed SR1 were observed under a light microscope at 7 dpt. After Dex treatment, SR1 did not show any histological changes (Fig. 6, SR1). The typical structure of epidermal layer (upper and lower), palisade mesophyll and spongy mesophyll cell layers were seen with some intercellular spaces. In comparison to SR1, CHLI-amiRNA transgenic line showed significant characteristics in leaf cell morphology. Even without Dex treatment, the palisade and spongy mesophyll cell layers were found to be swollen. In Dex-treated leaf tissues, however, a drastic reduction in chloroplast numbers in mesophyll cells and the disturbed arrangement of cell layers with lesser intercellular spaces was observed, suggesting that the induced silencing of CHLI gene affects the chloroplast biogenesis as well as the leaf morphogenesis.
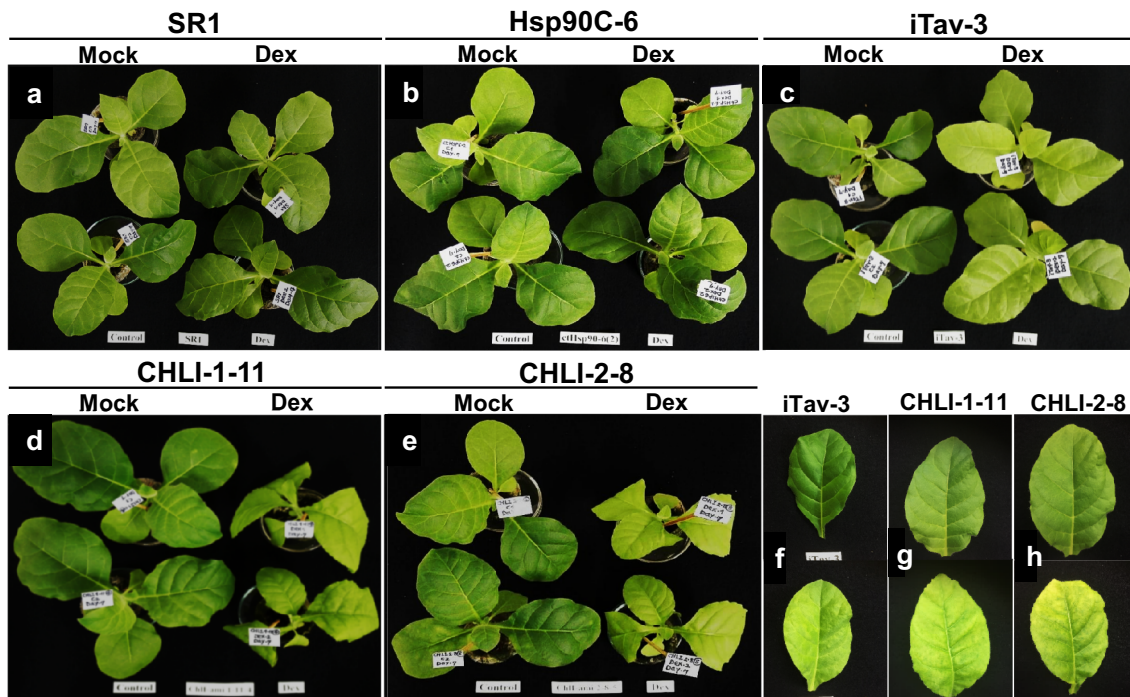
Fig. 4 Induced chlorosis observed in Dex-treated transgenic plants. Three-week-old plants were sprayed with 0.01% Tween-20 containing 2% ethanol (Mock) or 0.01% Tween-20 containing 50 μM Dex (2% solution of 2.5 mM stock in ethanol) (Dex) at an interval of 24 h until 7 days. **a** Non-transformed control SR1. **b** Control transformant Hsp90C-6. **c** iTav-3 as a positive control. **d, e** CHLI-1-11 and CHLI-2-8, representative CHLI-amiRNA-1 and -2 transgenic lines. **f, h** Close-up photographs of leaves with symptom-like phenotypes from Dex-treated plants (*lower panels*) and control leaves from mock-treated plants (*upper panels*). **f** A characteristic chlorosis with mosaic patterns in Dex-treated iTav-3. **g, h** Chlorosis in Dex-treated CHLI-1-11 and CHLI-2-8, respectively. The photographs were taken at 7 dpt (color in print)

CHLI-amiRNA induced chlorosis accompanies downregulation of other CPRGs and chaperone during early phase of chlorosis development

Studies of plants with chlorosis have reported the downregulation of CPRGs as a common phenomenon as mentioned in the introduction. To investigate whether the silencing of endogenous CHLI leads to the downregulation of other CPRGs, we performed expression analysis of ribulose-1,5-bisphosphate carboxylase/oxygenase small subunit (RSSU), light harvesting chlorophyll a/b binding protein (LHCa/b) and Hsp90C by qRT-PCR using EF1α mRNA as an endogenous reference. RSSU and LHCa/b were found to be significantly downregulated in CHLI-amiRNA transgenic lines at 2 dpt (Fig. 7a, b). By contrast, there was no significant decrease in Hsp90C expression levels in both CHLI-amiRNA transgenic lines (Fig. 7c). In iTav-3 plants, all three CPRGs were shown to significantly decreased in the expression levels (Fig. 7a–c). These results indicate that the expression of CPRGs are differentially affected during the chlorosis induced by different triggers, and suggest that Tav-induced chlorosis and that induced by CHLI silencing involve, at least in part, different pathways toward the loss of chlorophyll and chloroplast malfunctioning.

Induction of defense-related genes during the early phase of chlorosis induced by CHLI silencing

Previously, we have reported the induction of *PR1a* gene in iTav-tobacco plants shortly after the induced expression of CaMV-Tav transgene [41, 42]. Also, our recent study has demonstrated the drastic upregulation of *PR1a* gene during the chlorosis development in Hsp90C silenced transgenic tobacco [5]. To investigate whether it is the case in the present inducible chlorosis system with inducible CHLI silencing, we analyzed the expression of salicylic acid (SA)-responsive *PR1a*, ethylene-responsive *PR4* [6], and jasmonic acid (JA)-responsive *SAMDC* [28] at 2 dpt. Non-transformant SR1 and a control transformant Hsp90C-6 did not show activation of any defense-related genes upon Dex treatment (Fig. 8a–c). Consistently with our previous reports [41, 42], iTav-3 showed the upregulation of *PR1a* expression by 15-fold (Fig. 8a). Surprisingly, *PR1a* expression was upregulated by 258- and 1222-fold in CHLI-1-11 and CHLI-2-8 transgenic lines, respectively (Fig. 8a). *PR4* was upregulated by 2.0- 2.5 folds in CHLI-amiRNA transgenic lines but not in iTav-3 (Fig. 8b). Although the induction of *PR4* was observed in iTav-3 in our previous reports [5, 42], it was not observed in this study for some reason, suggesting that the induction of
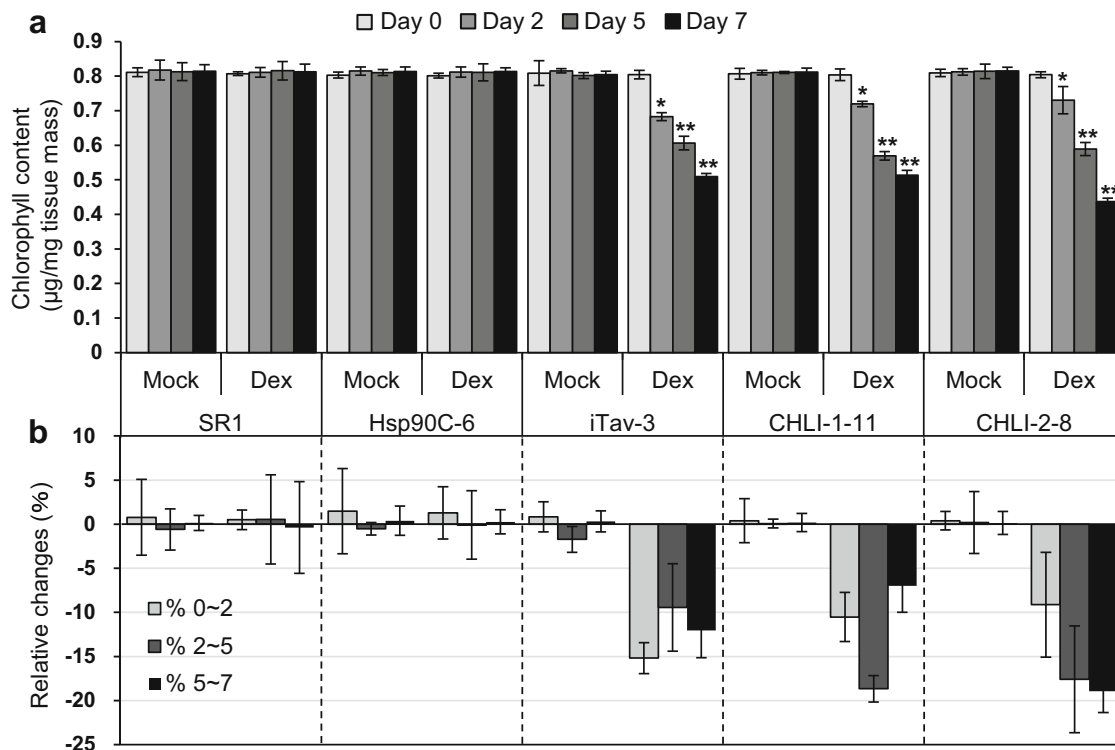
Fig. 5 Decrease in total chlorophyll content during the development of chlorosis in transgenic plants. Three-week-old plants were mock- or Dex-treated. Triplicate samples were collected from independent plants before (Day 0), and at 2, 5, and 7 dpt with Dex (Day 2, Day 5 and Day 7, respectively). The absorbance at various wavelength was measured, and total chlorophyll content was calculated. **a** Vertical bars presents the means of total chlorophyll content in three biological replicates ± standard deviation of mean values. *Single* and *double* *asterisks* indicate statistically significant difference between mock- and Dex-treated samples with $p < 0.05$ and $p < 0.01$, respectively in Student's *t* test. **b** Changes in chlorophyll content during early (from Day 0 to 2; % D 0–2), middle (from Day 2 to 5; % D 2–5), and late phases (from Day 5 to 7; % D 5–7) are shown in percentages to the mean values of Day 0 chlorophyll content with their standard deviations
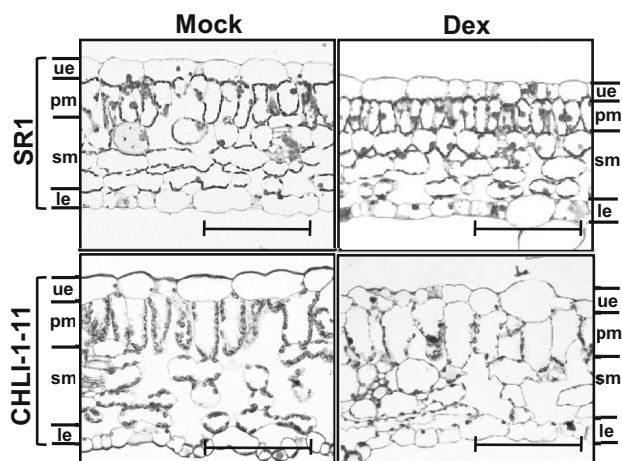

Fig. 6 Histological analysis of chlorotic leaf tissue from inducible CHLI-amiRNA transgenic plants. Leaf tissues from mock- and Dex-treated non-transformed control SR1, and CHLI-1-11 transgenic line were collected at 7 dpt. Transverse sections were observed under light microscope. *ue* upper epidermis, *pm* palisade mesophyll, *sm* spongy mesophyll, *le* lower epidermis. *Bar* = 20 μm

ethylene-responsive genes in iTav-3 could be affected by some growth condition. Because we observed clear chlorosis in iTav-3 in both previous and present study, the induction of *PR4* gene expression is unlikely to be crucial for the induction of chlorosis. The upregulation of *SAMDC* was observed only in CHLI-1-11 transgenic line (Fig. 8c). These results collectively indicate that in the inducible chlorosis system with CHLI silencing, some defense-related genes are upregulated during the development of chlorosis, despite that the system does not involve any pathogen-derived molecules.

Discussion

In the present study, we established an inducible system that expresses amiRNA targeting CHLI mRNA. In this system, CHLI mRNA levels and total chlorophyll content decreased significantly in 2 days, resulting in the development of visible chlorosis in 5 days. The present results
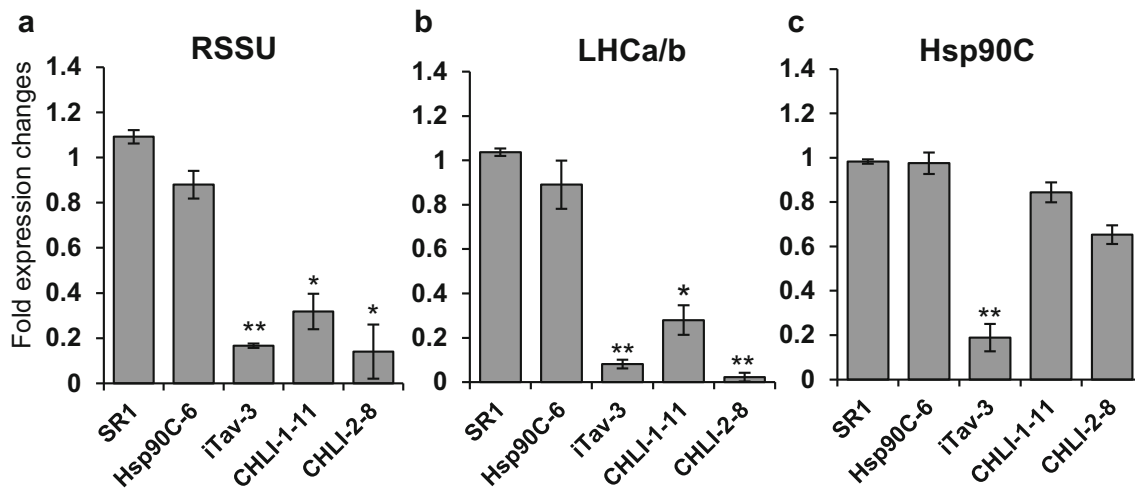
Fig. 7 Expression analysis of CPRGs and chloroplast chaperone by qRT-PCR. Non-transformed control (SR1), transformed control Hsp90C-6, and three transgenic lines with inducible chlorosis, iTav-3, CHLI-1-11, and CHLI-2-8 were mock- or Dex-treated for 2 days and the expression of RSSU (**a**), LHCa/b (**b**), and Hsp90C (**c**) was analyzed by qRT-PCR in triplicate. The expression of target genes was normalized to NtEF1α. The fold expression changes were calculated in chlorotic leaf samples by comparing their relative expression with mock treated. The mean values of three biological replications and standard error of means are shown. The *single* and *double asterisks* show statistically significant difference between mock- and Dex-treated plants with $p < 0.05$ and $p < 0.01$, respectively in Student's *t* test
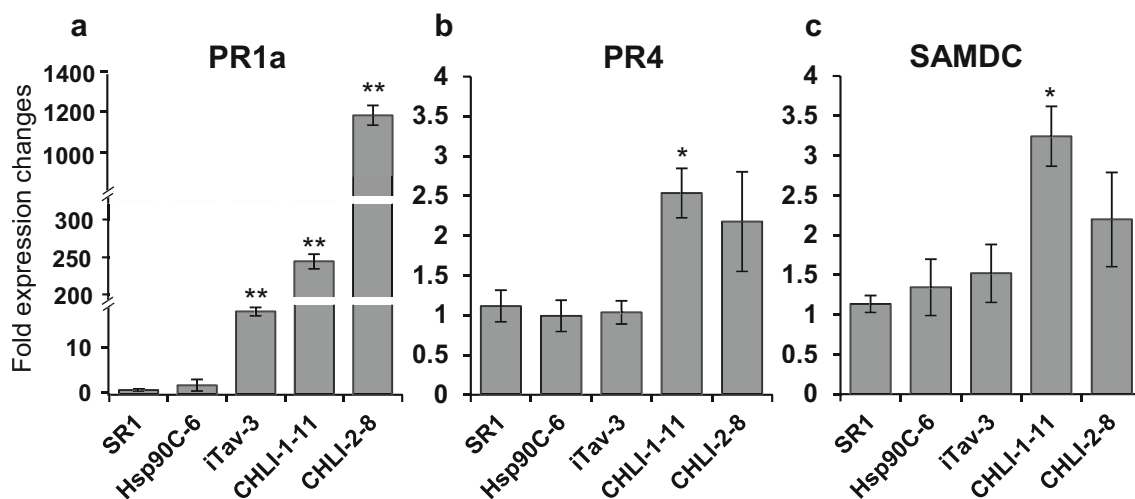
Fig. 8 Expression analysis of plant defense genes by qRT-PCR. Non-transformed control (SR1), transformed control, Hsp90C-6, and three transgenic lines, iTav-3, CHLI-1-11, and CHLI-2-8 were mock- or Dex-treated until 2 days and expression of PR1a (**a**), PR4 (**b**), and SAMDC (**c**) was analyzed by qRT-PCR in triplicate. The expression of target genes was normalized to NtEF1α. The fold expression changes were calculated in chlorotic leaf samples by comparing their relative expression with mock treated. The mean values of three biological replications and standard error of means are shown. The *single* and *double asterisks* show statistically significant difference between mock- and Dex-treated plants with $p < 0.05$ and $p < 0.01$, respectively in Student's *t* test

are consistent with previous studies on the Y-sat-mediated pathogenesis of CMV [34, 35]. Similar chlorosis phenotypes were also observed in *Arabidopsis thaliana* [30] and *Zea mays* [31] mutants, and in CHLI-silenced transgenic tobacco plants [26]. The present experimental system has an advantage over the virus-infected plants, mutants, and the constitutively silenced transgenic plants in that it enables us to analyze early phase of chlorosis development, as manifested by the decreased chlorophyll content, the downregulation of CPRGs expression, and the induction of defense-related genes at 2 dpt, when the plants had not shown any visible sign of chlorosis development. As with the previously reported inducible chlorosis systems, iTav tobacco [42] and Hsp90C-hpRNA transgenic plants [5], the present system would also serve as a promising tool to analyze precise mechanisms leading to leaf chlorosis.

In this study, we selected two transgenic lines, CHLI-1-11 and CHLI-2-8. After Dex treatment, these lines

produced a severe leaf chlorosis with green dots on leaf blades, growth suppression, shrinking of leaves and a significant decrease in total chlorophyll content (Fig. 4). The results of chlorophyll content reduction in CHLI-amiRNA expressing transgenic lines were in agreement with previously reported in *Arabidopsis ChlI* mutants, *ch42-1* and *-3* [30] and CHLI-silenced transgenic tobacco plants [26]. The differences in symptom severity and the decrease in chlorophyll content were observed between CHLI-1-11 and CHLI-2-8, which might be due to the difference in the degree of silencing. This notion is supported by the expression analysis by qRT-PCR. The positive correlation between the downregulation of CHLI expression levels and symptom severity would reinforce our conclusion that the downregulation of CHLI expression caused the chlorosis. However, it is still unclear whether or not the difference in the nucleotide sequence of two amiRNAs, CHLI-ami-1 and -2, is responsible for the difference in the magnitude of silencing.

The expression analysis of CPRGs revealed that other CPRGs—RSSU and LHCa/b—were strongly downregulated in Dex-treated CHLI-amiRNA expressing transgenic lines at 2 dpt. In addition, a drastic elevation of *PR1a* expression levels was observed in both CHLI-amiRNAs expressing lines. Taken together, these results strongly suggest that the silencing of CHLI induces chlorosis, not through the simple decrease of chlorophyll biosynthesis but the activation of some plant responses. We have found the downregulation of CPRGs expression and the induction of *PR1a* expression in transgenic plants expressing Hsp90C-hpRNA [5] as well as in iTav-tobacco plants [41, 42]. The present results and these reports collectively suggest that a rapid downregulation of CPRGs and a rapid upregulation of defense-related genes are common pathways of chlorosis development.

Although the downregulation of CPRGs was shown to be a common event in two inducible silencing systems—CHLI-amiRNA– and Hsp90C-hpRNA–expressing transgenic plants—, the mechanism underlying these downregulation events remains to be studied. The findings are consistent with the previous observation in CHLI-silenced transgenic tobacco plants [26]. The silencing of Thioredoxin-F and M, which interact with and support the enzymatic activity of CHLI, resulted in the reduced expression of CPRGs and the chlorotic phenotype in pea plants [18]. Although the evidence is indirect in this case, it may support the idea that the downregulation of CHLI gives rise to the reduced expression of CPRGs. The gene encoding CHLH subunit of Mg-chelatase has been identified as the causal gene of *Arabidopsis gun5* mutant, which expresses CPRGs in the absence of chloroplast development [20], suggesting that perturbations of the tetrapyrrole biosynthetic pathway generate a signal from chloroplasts to

the nucleus for regulating CPRGs. However, they also provided evidence that ChlI subunit of Mg-chelatase is not necessary for plastid signal transduction. Perturbations in tetrapyrrole biosynthesis and accumulation of tetrapyrrole intermediate, Mg-protoporphyrin IX, have been shown to negatively regulate the expression of nuclear genes encoding photosynthetic proteins in both algae and higher plants [15, 36–39]. It is noteworthy that the Mg-Protoporphyrin IX signal is reported to be received by CUF elements in *LHCa/b* gene promoter and to lead the gene to downregulation [36]. Although the silencing of CHLI is most likely to play a major role in Y-sat–mediated CMV pathogenesis, the retrograde signaling systems would also have roles in the development of chlorosis. The inducible and synchronous system presented in this report would help us analyze the involvement of the retrograde signaling systems in the chlorosis development. Also, we propose that this system could be useful for studying the regulation of chlorophyll biosynthesis and chloroplast biogenesis.

Unlike other CPRGs, the expression of chloroplast molecular chaperone Hsp90C remained unaffected in our CHLI-silenced transgenic plants whereas it was downregulated to a greater extent in iTav-tobacco plants. Because Hsp90C has an essential role in protein transport into chloroplasts, the silencing of this gene could affect varying processes of chloroplast biogenesis [14]. By contrast, CHLI has a role only in chlorophyll synthesis, and therefore, the silencing of this gene would have a limited impact on chloroplast biogenesis. Although the Hsp90C genes have been shown to be a pathogenic target of PLMVd [22] and their silencing resulted in chlorosis development in transgenic tobacco [5], the downregulation of the Hsp90C genes is unlikely to be one of the leading causes of chlorosis development in CHLI-silenced plants.

A drastic increase in *PR1a* expression was observed in CHLI-amiRNAs expressing plants as previously reported for Hsp90C-hpRNA transgenic plants [5], suggesting that the *PR1a* gene activation is a common downstream event of the silencing of both Hsp90C and CHLI. Although the activation of SA pathway is anticipated in these two experimental systems, it remains unknown what in those transgenic plants activate the *PR1a* gene in the absence of any pathogen-derived molecules. Possible mechanisms underlying the *PR1a* gene activation would be the production of ROS in the chloroplast of CHLI-silenced plants. As discussed before, CHLI-silencing could give rise to the accumulation of chlorophyll biosynthesis intermediate Mg-protoporphyrin IX, which reportedly produces $^1O_2$ in plants [40]. Increased accumulation of ROS inside the chloroplast would give rise to the elevated level of SA [11], which activates *PR1a* gene. On the contrary, we reported that the *PR1a* would be induced in Dex-treated iTav-tobacco plants through an SA-independent manner [41]. The upregulation

of *PR1a* gene expression was much higher in CHLI-amiRNAs and Hsp90C-hpRNA transgenic plants than in iTav-tobacco. Therefore, it is also possible that the mode of *PR1a* induction in iTav-tobacco differs from those in CHLI- and Hsp90C-silenced plants. It is of great importance to analyze comparatively the SA production in these three inducible chlorosis systems for elucidating the precise molecular mechanisms underlying the chlorosis development.

It should be noted that we found some morphological abnormalities in the leaf tissues of CHLI-amiRNA transgenic lines. In comparison with SR1, the Dex untreated CHLI-1-11 showed slight morphological defects, which could result from a leaky expression of the transgene [42] and a mild silencing of CHLI gene expression. However, it is unknown how the mild silencing of CHLI gene in those transgenic plants affects leaf tissue morphology. Unless treated with Dex, CHLI-amiRNA transgenic lines are healthy: they showed a comparable chlorophyll content to untransformed SR1 plants, passed through the developmental stages and finally bore seeds. In contrast, they developed clear chlorosis after Dex treatment, which enables us to study the processes during the development of chlorosis. Nonetheless, because of the aforementioned mild effect from the uninduced transgene, Dex-treated and -untreated non-transformed control plants should be analyzed in parallel with the transgenic plants in the future study as we have done in this report.

Expression of CHLI-targeting amiRNAs under the control of a chemically inducible promoter enabled us to establish a novel inducible chlorosis system. Basic characterization of this systems suggested that a rapid downregulation of CPRGs and a rapid upregulation of defense-related genes are common pathways of chlorosis development as the previously reported systems did [5, 42]. In-depth comparative analyses of the regulation of CPRGs and defense-related genes, including the quantitative kinetic analysis of defense-related phytohormones, in these three inducible chlorosis systems would lead us to a better understanding of the mechanism underlying the chlorosis.

References

1. Almon E, Horowitz M, Wang HL, Lucas WJ, Zamski E, Wolf S. Phloem-specific expression of the *Tobacco mosaic virus* movement protein alters carbon metabolism and partitioning in transgenic potato plants. Plant Physiol. 1997;115:1599–607.
2. Aoyama T, Chua NH. A glucocorticoid-mediated transcriptional induction system in transgenic plants. Plant J. 1997;11:605–12.
3. Balachandran S, Osmond CB, Daley PF. Diagnosis of the earliest strain-specific interactions between Tobacco mosaic virus and chloroplasts of tobacco leaves in vivo by means of chlorophyll fluorescence imaging. Plant Physiol. 1994;104:1059–65.
4. Bhat S, Folimonova SY, Cole AB, Ballard KD, Lei Z, Watson BS, Sumner LW, Nelson RS. Influence of host chloroplast proteins on *Tobacco mosaic virus* accumulation and intercellular movement. Plant Physiol. 2012;161:134–47.
5. Bhor SA, Tateda C, Mochizuki T, Sekine KT, Takashi Y, Yamaoka Y, Nishiguchi M, Kobayashi K. Inducible transgenic tobacco system to study the mechanisms underlying chlorosis mediated by the silencing of chloroplast heat shock protein 90. VirusDis. 2017. doi:10.1007/s13337-017-0361-0.
6. Biondi S, Scaramagli S, Capitani F, Altamura MM, Torrigiani P. Methyl jasmonate upregulates biosynthetic gene expression, oxidation and conjugation of polyamines, and inhibits shoot formation in tobacco thin layers. J Exp Bot. 2001;52:231–42.
7. Christov I, Stefanov D, Velinov T, Goltsev V, Georgieva K, Abracheva P, Genova Y, Christov N. The symptomless leaf infection with *Grapevine leaf roll associated virus 3* in grown in vitro plants as a simple model system for investigation of viral effects on photosynthesis. J Plant Physiol. 2007;164:1124–33.
8. Dardick C. Comparative expression profiling of *Nicotiana benthamiana* leaves systemically infected with three fruit tree viruses. Mol Plant Microbe Interact. 2007;20:1004–17.
9. Guo DP, Guo YP, Zhao JP, Liu H, Peng Y, Wang QM, Chen JS, Rao GZ. Photosynthetic rate and chlorophyll fluorescence in leaves of stem mustard (*Brassica juncea* var. *tsatsai*) after turnip mosaic virus infection. Plant Sci. 2005;168:57–63.
10. Herbers K, Takahata Y, Melzer M, Mock HP, Hajirezaei M, Sonnewald U. Regulation of carbohydrate partitioning during the interaction of Potato virus Y with tobacco. Mol Plant Pathol. 2000;1:51–9.
11. Herrera-Vasquez A, Salinas P, Holuigue L. Salicylic acid and reactive oxygen species interplay in the transcriptional control of defense genes expression. Front Plant Sci. 2015;. doi:10.3389/fpls.2015.00171.
12. Horsch RB, Fry JE, Hoffmann NL, Wallroth M, Eichholtz D, Rogers SG. A simple method for transferring genes into plants. Science. 1985;227:1229–31.
13. Hu CC, Hsu YH, Lin NS. Satellite RNAs and satellite viruses of plants. Viruses. 2009;1:1325–50.
14. Inoue H, Li M, Schnell DJ. An essential role for chloroplast heat shock protein 90 (Hsp90C) in protein import into chloroplasts. Proc Natl Acad Sci USA. 2013;110(8):3173–8.
15. Johanningmeier U, Howell SH. Regulation of light-harvesting chlorophyll-binding protein mRNA accumulation in *Chlamydomonas reinhardi*. J Biol Chem. 1984;259(21):13541–9.
16. Kyseláková H, Prokopová J, Nauš J, Novák O, Navrátil M, Šafářová D, Špundová M, Ilik P. Photosynthetic alterations of pea leaves infected systemically by Pea enation mosaic virus: a coordinated decrease in efficiencies of CO_2 assimilation and photosystem II photochemistry. Plant Physiol Biochem. 2011;49:1279–89.
17. Lehto K, Tikkanen M, Hiriart J-B, Paakkarinen V, Aro E-M. Depletion of the photosystem II core complex in mature tobacco leaves infected by the *flavum* strain of *Tobacco mosaic virus*. Mol Plant Microbe Interact. 2003;16:1135–44.
18. Luo T, Fan T, Liu Y, Rothbart M, Yu J, Zhou S, Grimm B, Luo M. Thioredoxin redox regulates ATPase activity of magnesium chelatase CHLI subunit and modulates redox-mediated signaling

in tetrapyrrole biosynthesis and homeostasis of reactive oxygen species in pea plants. Plant Physiol. 2012;159:118–30.

19. Manfre A, Glenn M, Nuñez A, Moreau RA, Dardick C. Light quantity and photosystem function mediate host susceptibility to *Turnip mosaic virus* via a salicylic acid-independent mechanism. Mol Plant Microbe Interact. 2011;24:315–27.

20. Mochizuki N, Brusslan JA, Larkin R, Nagatani A, Chory J. *Arabidopsis genomes uncoupled 5 (GUN5)* mutant reveals the involvement of Mg-chelatase H subunit in plastid-to-nucleus signal transduction. Proc Natl Acad Sci USA. 2001;98:2053–8.

21. Mochizuki T, Ogata Y, Hirata Y, Ohki ST. Quantitative transcriptional changes associated with chlorosis severity in mosaic leaves of tobacco plants infected with *Cucumber mosaic virus*. Mol Plant Pathol. 2014;15:242–54.

22. Navarro B, Gisel A, Rodio ME, Delgado S, Flores R, Di Serio F. Small RNAs containing the pathogenic determinant of a chloroplast- replicating viroid guide the degradation of a host mRNA as predicted by RNA silencing. Plant J. 2012;70:991–1003.

23. Olesinski AA, Almon E, Navot N, Perl A, Galun E, Lucas WJ, Wolf S. Tissue-specific expression of the Tobacco mosaic virus movement protein in transgenic potato plants alters plasmodesmal function and carbohydrate partitioning. Plant Physiol. 1996;111:541–50.

24. Ossowski S, Schwab R, Weigel D. Gene silencing in plants using artificial microRNAs and other small RNAs. Plant J. 2008;53:674–90.

25. Otulak K, Chouda M, Bujarski J, Garbaczewska G. The evidence of *Tobacco rattle virus* impact on host plant organelles ultrastructure. Micron. 2015;70:7–20.

26. Papenbrock J, Pfündel E, Mock HP, Grimm B. Decreased and increased expression of the subunit CHL I diminishes Mg chelatase activity and reduces chlorophyll synthesis in transgenic tobacco plants. Plant J. 2000;22:155–64.

27. Porra RJ, Thompson WA, Kriedemann PE. Determination of accurate extinction coefficients and simultaneous-equations for assaying chlorophyll *a* and chlorophyll *b* extracted with four different solvents: verification of the concentration of chlorophyll standards by atomic-absorption spectroscopy. Biochim Biophys Acta. 1989;975:384–94.

28. Qin J, Zuo K, Zhao J, Ling H, Cao Y, Qiu C, Li F, Sun X, Tang K. Overexpression of *GbERF* confers alteration of ethylene-responsive gene expression and enhanced resistance to *Pseudomonas syringae* in transgenic tobacco. J Biosci. 2006;31:255–63.

29. Rahoutei J, García-Luque I, Barón M. Inhibition of photosynthesis by viral infection: effect on PSII structure and function. Physiol Plant. 2000;110:286–92.

30. Rissler HM, Collakova E, DellaPenna D, Whelan J, Pogson BJ. Chlorophyll biosynthesis. Expression of a second *Chl I* gene of

magnesium chelatase in Arabidopsis supports only limited chlorophyll synthesis. Plant Physiol. 2002;128:770–9.

31. Sawers RJH, Viney J, Farmer PR, Bussey RR, Olsefski G, Anufrikova K, Hunter N, Brutnell TP. The maize *Oil Yellow1 (Oy1)* gene encodes the I subunit of magnesium chelatase. Plant Mol Biol. 2006;60:95–106.

32. Schwab R, Ossowski S, Riester M, Warthmann N, Weigel D. Highly specific gene silencing by artificial microRNAs in *Arabidopsis*. Plant Cell. 2006;18:1121–33.

33. Shi Y, Chen J, Hong X, Chen J, Adams MJ. A potyvirus P1 protein interacts with the Rieske Fe/S protein of its host. Mol Plant Pathol. 2007;8:785–90.

34. Shimura H, Pantaleo V, Ishihara T, Myojo N, Inaba J-I, Sueda K, Burgyán J, Chikara M. A viral satellite RNA induces yellow symptoms on tobacco by targeting a gene involved in chlorophyll biosynthesis using the RNA silencing machinery. PLoS Pathog. 2011;7:1–12.

35. Smith NA, Eamens AL, Wang MB. Viral small interfering RNAs target host genes to mediate disease symptoms in plants. PLoS Pathog. 2011;7:1–9.

36. Strand Å, Asami T, Alonso J, Ecker JR, Chory J. Chloroplast to nucleus communication triggered by accumulation of Mg-protoporphyrin IX. Nature. 2003;5:79–83.

37. Strand Å. Plastid-to-nucleus signalling. Curr Opin Plant Biol. 2004;7:621–5.

38. Surpin M, Larkin RM, Chory J. Signal transduction between the chloroplast and the nucleus. Plant Cell. 2002;14:S327–38.

39. Susek RE, Ausubel FM, Chory J. Signal transduction mutants of Arabidopsis uncouple nuclear *CAB* and *RBCS* gene expression from chloroplast development. Cell. 1993;74:787–99.

40. Tripathy BC, Oelmüller R. Reactive oxygen species generation and signaling in plants. Plant Signal Behav. 2012;7:1621–33.

41. Waliullah S, Kosaka N, Yaeno T, Ali ME, Sekine K-T, Atsumi G, Yamaoka N, Nishiguchi M, Takahashi H, Kobayashi K. *Cauliflower mosaic virus* Tav protein induces leaf chlorosis in transgenic tobacco through a host response to virulence function of Tav. J Gen Plant Pathol. 2015;81:261–70.

42. Waliullah S, Mochizuki T, Sekine K-T, Atsumi G, Ali ME, Yaeno T, Yamaoka N, Nishiguchi M, Kobayashi K. Artificial induction of a plant virus protein in transgenic tobacco provides a synchronous system for analyzing the process of leaf chlorosis. Physiol Mol Plant Pathol. 2014;88:43–51.

43. Yang J, Zhang F, Li J, Chen JP, Zhang HM. Integrative analysis of the microRNAome and transcriptome illuminates the response of susceptible rice plants to Rice stripe virus. PLoS ONE. 2016;11:1–21.

44. Zhao J, Zhang X, Hong Y, Liu Y. Chloroplast in plant-virus interaction. Front Microbiol. 2016;7:1–20.